

Hsp90 inhibitor NMS-E973 exerts the anticancer effect against glioblastoma via induction of PUMA-mediated apoptosis

Libo Sun¹
Shoujun Yang²
Guonan Chi¹
Xingyi Jin¹

¹First Department of Neurosurgery, China-Japan Union Hospital of Jilin University, Changhun, Jilin, People's Republic of China; ²Department of Rehabilitation, China-Japan Union Hospital of Jilin University, Changhun, Jilin, People's Republic of China

Background: Glioblastoma is one of the most aggressive and common malignancies of the central nervous system in humans. Owing to the correlation of high Hsp90 expression with prognosis and clinical pathology features of diverse types of cancer, targeting Hsp90 with small-molecule inhibitors has become a promising anticancer strategy.

Purpose: In this study, we aimed to explore the possibility of anticancer effect of NMS-E973 in glioblastoma and elucidate the mechanism.

Methods: Cell based MTT assay and colony formation assay were used to detect cell viability. Apoptosis was analyzed by nuclear staining with Hoechst 33258 and Annexin V/propidium iodide staining followed by flow cytometry. Western-blot and RT-PCR were used to detect gene expression. Xenograft assay was used to explore the anticancer effect of NMS-E973 in vivo.

Results: We found that NMS-E973 induces apoptosis and inhibits cell growth in glioblastoma cells in cell culture and xenograft models. As a proapoptotic Bcl-2 member, PUMA was induced by NMS-E973 in a p53-dependent manner in glioblastoma in cell culture, thereby inducing apoptosis in glioblastoma cells. Furthermore, PUMA was induced by NMS-E973 treatment in xenograft tumors, and deficiency in PUMA significantly suppressed the antitumor effects of NMS-E973.

Conclusion: Our study suggests that PUMA-mediated apoptosis is important for the therapeutic responses of NMS-E973. Induction of PUMA might be a potential biomarker for predicting NMS-E973 responses.

Keywords: NMS-E973, PUMA, glioblastoma, apoptosis

Introduction

As one of the most aggressive and common malignancies of the central nervous system in humans, glioblastoma represents the second leading cause of cancer-related mortality in children under the age of 15 and the fourth leading cause in adults between the age of 15 and 34 throughout the world.^{1,2} Given the difficulty in removing glioblastoma tumor cell infiltrating or migrating to surrounding brain tissues by surgery, as well as owing to the high invasiveness of glioblastoma tumor cell and its resistance to conventional chemotherapy and radiation therapy, glioblastoma patients usually have a 1-year median survival time, which rises to 15% and 2% after 2 and 3 years, respectively.³⁻⁸ Therefore, exploring new therapies and understanding the molecular mechanism of its action is desirable.

Hsp90 has been shown to behave as a molecular chaperone for regulating degradation, folding, and maturation of client proteins in eukaryotes.⁹ Owing to the correlation of high Hsp90 expression with prognosis and clinicopathologic features of diverse types of cancer, targeting Hsp90 with small-molecule inhibitors has become a promising anticancer strategy.¹⁰⁻¹² NMS-E973 is a recently developed Hsp90 inhibitor that

Correspondence: Xingyi Jin
First Department of Neurosurgery,
China-Japan Union Hospital of Jilin
University, Changhun, Jilin 130033,
People's Republic of China
Tel +86 0431 8499 5933
Email xyjin@jlu.edu.cn

belongs to isoxazole-derived class.¹³ A previous study suggested that NMS-E973 single treatment displayed significant efficacy in a human ovarian A2780 xenograft tumor model, while combined treatment with HO-1 inhibitor demonstrated potential anticancer efficacy in melanoma.^{14,15} However, research focused on the effect of NMS-E973 in glioblastoma and its potential mechanism of action is lacking.

In this study, we aimed to evaluate the antitumor efficacy of NMS-E973 in glioblastoma both in vitro and in vivo. This study also elucidates the mechanism underlying NMS-E973-induced apoptosis in glioblastoma.

Materials and methods

Cell culture and reagents

Human glioblastoma cell lines (U87 and SW1088) and human embryonic kidney cells 293T were purchased from the Type Culture Collection of the Chinese Academy of Sciences (Shanghai, People's Republic of China) were maintained in Dulbecco's Modified Eagle's Medium (GIBCO, Shanghai, People's Republic of China) supplemented with 10% fetal bovine serum, 100 U/mL penicillin, and 100 mg/mL streptomycin, and were incubated at 37°C in a humidified incubator supplemented with 5% CO₂. NMS-E973 was purchased from Selleck (Houston, TX, USA).

Analysis of cell viability and apoptosis

MTT was utilized to detect cell viability according to the manufacturer's instructions. Briefly, the cells were seeded in 96-well culture plates and incubated at 37°C with 5% CO₂ for 72 hours. For the colony formation assay, 5,000 cells were plated in a six-well plate for 12 days. Colonies were subjected to methanol/acetone (1:1) fixation and stained with crystal violet.

Apoptosis was analyzed by nuclear staining with Hoechst 33258 (Invitrogen, Carlsbad, CA, USA), and Annexin V/propidium iodide (Invitrogen) staining followed by flow cytometry. The percentage of Annexin V+ cells (indicated in the two right quadrants) was plotted.

Real-time reverse-transcriptase (RT) PCR

Total RNA was extracted with Mini RNA Isolation II Kit from Zymo Research, and the procedure was performed in accordance with the provided protocol. Then the Super Script II reverse transcriptase was utilized to create cDNA from the total RNA. Real-time PCR was carried out as described earlier.¹⁶ The following primers were used for *PUMA*: forward: 5'-CGA CCT CAA CGC ACA GTA CGA-3', reverse: 5'-AGG CAC CTA ATT GGG CTC CAT-3', *BID*: forward: 5'-GGA GAC GAG TTT AAC GCT TAC-3', reverse: 5'-CAA GCA AAA TGT CTG CAT GG-3', *NOXA*: forward:

5'-GCT GGA AGT CGA GTG TGC TA-3', reverse: 5'-CCT GAG CAG AAG AGT TTG GA-3', *BAD*: forward: 5'-CGG AGG ATG AGT GAC GAG TT-3', reverse: 5'-GAT GTG GAG CGA AGG TCA CT-3', and β -*actin*: forward: 5'-GAC CTC ACA GAC TAC CTC AT-3', reverse: 5'-AGA CAG CAC TGT GTT GGC TA-3'.

si RNA knockdown

Transfection was performed 24 hours before NMS-E973 treatment using 200 pmol of siRNA in 1 well of a 12-well plate. siRNA against PUMA (ACGTGTGACCACTGGCATTdtdT) was synthesized by GenePharma (Shanghai, People's Republic of China) and transfected with Lipofectamine 2000 (Invitrogen) according to the manufacturer's instructions.

Generation of stable cell line (U87-PUMA-KD)

The lentiviral plasmid pSicoR PGK puro (GeneCopoeia, Rockville, MD, USA) expressing shRNA against PUMA and Lenti-Pac HIV Expression Packaging mix (GeneCopoeia) were cotransfected into 293T cells using Lipofectamine 2000 (Invitrogen). After transfection for 48 hours, lentiviral particles were harvested and then transduced into the U87 glioblastoma cells, and the stably transfected cells were selected using puromycin and validated by RT-PCR and Western blot to confirm successful PUMA knockdown.

Detection of Activated caspase-3, -9, and -8

After NMS-E973 treatment, cell lysates (50 μ g) were incubated with 200 nM Ac-DEVD-AFC, Ac-IETD-AFC, and Ac-LEHD-AFC (caspase-3, -8, and -9, respectively; Cayman Chemical, Ann Arbor, MI, USA) in a buffer solution comprising 20 mM HEPES at pH 7.4, 100 mM NaCl, 0.1% CHAPS, DTT (10 mM), and ND 10% of sucrose at 37°C for 60 minutes. The incubation process was closely controlled and measured with fluorescence emission and excitation at 535 and 405 nm each.

Western blot analysis

Western blotting was performed according to the standard protocol with primary antibodies against PUMA, NOXA, BID, and cleaved caspase-3, -9, and -8; and β -actin was used as an internal control. All primary antibodies were purchased from Cell Signaling (Beverly, MA, USA).

Xenograft studies

All animal experiments were approved by China-Japan Union Hospital of Jilin University Animal Care and Use

Committee, and all experiments followed the United Kingdom Coordinating Committee for Cancer Research guidelines regarding the welfare of the animals. 2×10^6 U87 or U87-PU-MA-KD cells were injected subcutaneously into the dorsal flank of BALB/c nude mice. After implantation, tumors were allowed to grow for 7 days before treatment was initiated. Mice were randomized into one of two groups ($n=6$ per group), one receiving vehicle (saline), and the other NMS-E973 (25 mg/kg/d) on days 1–7. Six mice were included in one experimental group. Tumor diameters were measured every 2 days, and tumor volumes were calculated ($\text{width}^2 \times \text{length} \times 0.5$). Mice were euthanized when tumors reached $\sim 1 \text{ cm}^3$ in size.

Statistical analysis

Statistical analyses were carried out using GraphPad Prism IV software (GraphPad Software, La Jolla, CA, USA). Student's *t*-test was used to analyze the results, expressed as mean \pm SD. If $P < 0.05$, differences were considered significant.

Results

Effect of NMS-E973 on the viability of glioblastoma cells

In order to determine the antitumor activity of NMS-E973 against glioblastoma, we measured the cell growth in two glioblastoma cells by MTT assay. As shown in Figure 1A, 0.01 μM NMS-E973 treatment barely impacted cell viability in U87 cells. From 0.1 μM , NMS-E973 treatment clearly resulted in a decrease in the viability of U87 cells, which reached $>90\%$ at 10 μM . A similar dose-dependent decrease in cell viability in SW1088 cells was also observed after treatment with NMS-E973 (Figure 1B). The median lethal dose value of NMS-E973 was similar between U87 and SW1088 cells, around 1 μM . Furthermore, the long-term colony formation capacities of these two glioblastoma cells after exposure to NMS-E973 were measured with crystal violet staining. We found that the colony size in NMS-E973 treatment group was smaller than in the untreated group

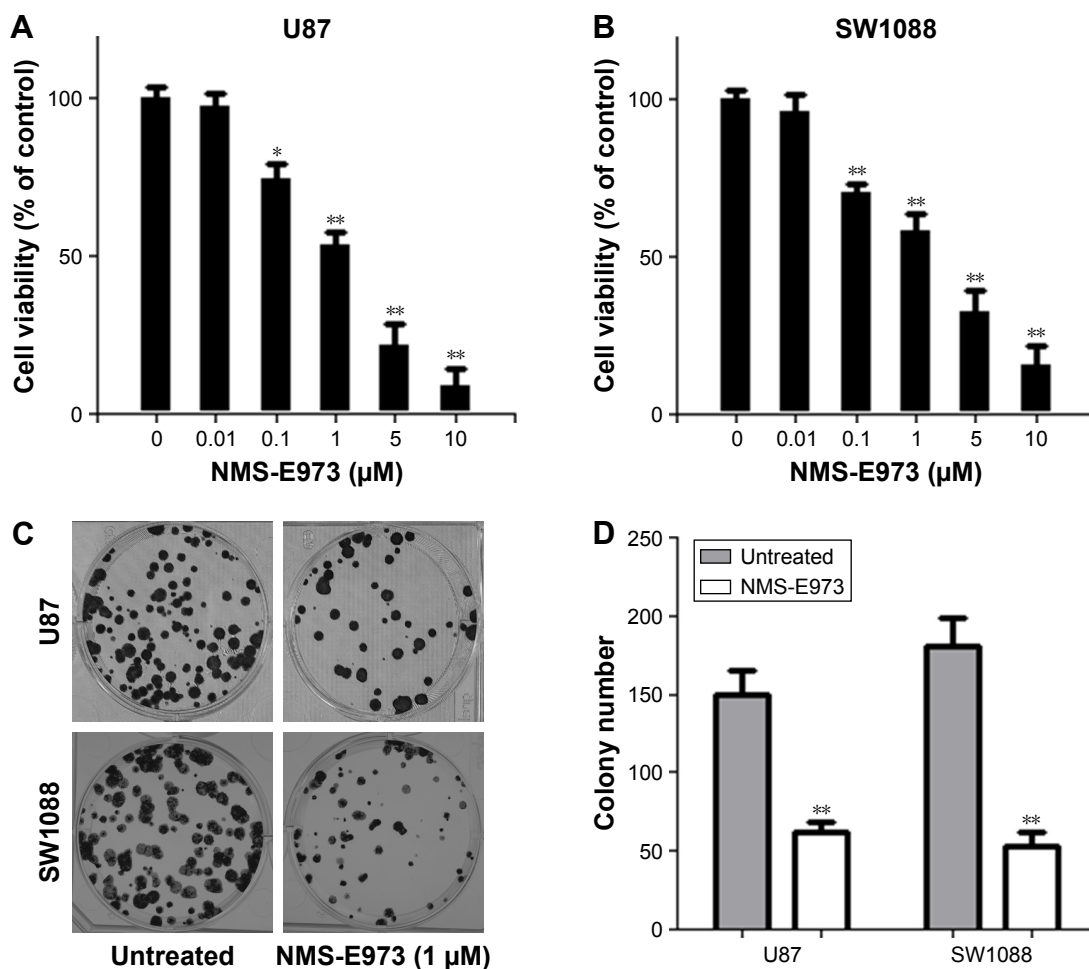


Figure 1 Effect of NMS-E973 on the viability of glioblastoma cells.

Notes: (A) U87 and (B) SW1088 cells were treated with NMS-E973 for 72 hours. Cell viability was measured by MTT assay. (C) Representative images of colony formation assay in U87 and SW1088 cells after exposure to NMS-E973. (D) Quantification of colony numbers in the colony formation assay. Expression of significant difference: * $P < 0.01$; ** $P < 0.001$.

(Figure 1C). Compared to untreated group, NMS-E973-treated cells had a significantly less colony number in both U87 and SW1088 cells (Figure 1C and D).

NMS-E973 induces apoptosis in glioblastoma cells

To explore if the effect of NMS-E973 on the viability of glioblastoma cells is attributed to induction of apoptosis, glioblastoma cells were treated with the median lethal dose value of NMS-E973 as measured earlier, which is 1 μ M. First, we found that the number of cells with condensed chromatin and micronucleation following nuclear staining with Hoechst 33258 was significantly increased after 48 hours of NMS-E973 treatment in both U87 and

SW1088 cells (Figure 2A and B). Second, Annexin V/propidium iodide staining showed that 48-hour NMS-E973 treatment induced over 30% Annexin V+ cells in both the glioblastoma cell lines (Figure 2C and D). Third, activation of caspase-3, -9, and -8 was also observed in both U87 and SW1088 cells after NMS-E973 treatment from 4 to 24 hours (Figure 3).

PUMA is induced by NMS-E973 in glioblastoma cells in a p53-dependent manner

In order to understand the mechanism underlying NMS-E973-induced apoptosis in glioblastoma cells, several Bcl-2 family protein expressions were analyzed using qRT-PCR

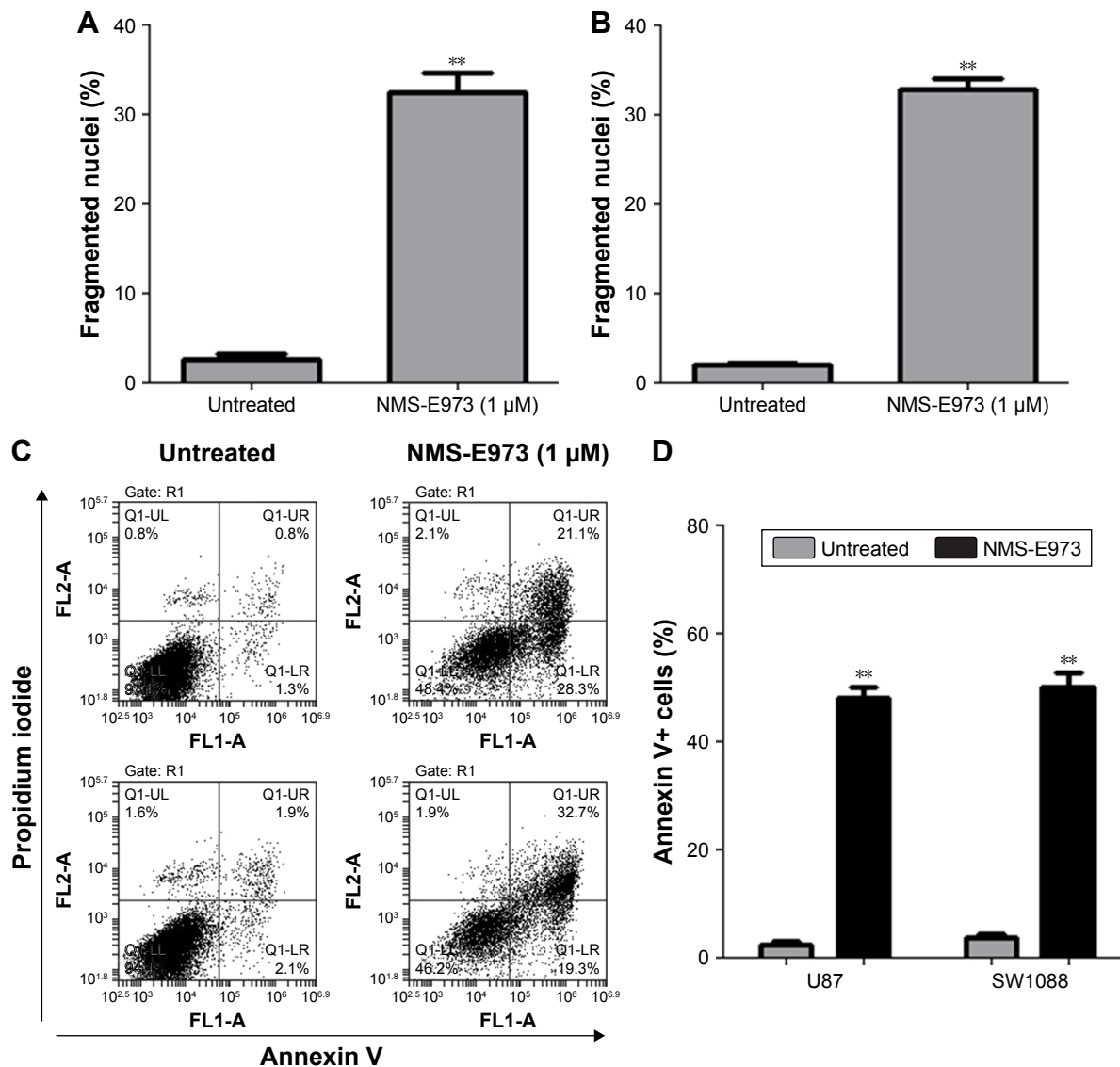


Figure 2 NMS-E973 induces apoptosis in glioblastoma cells.

Notes: (A) U87 and (B) SW1088 cells were treated with NMS-E973 (1 μ M) for 2 days. The number of condensed and fragmented nuclei was counted for apoptosis analysis. (C) Representative images of Annexin V/propidium iodide staining in U87 and SW1088 cells after exposure to NMS-E973. (D) Annexin V+ cell percentage (indicated in the two right quadrants) was plotted. Expression of significant difference: ** $P < 0.001$.

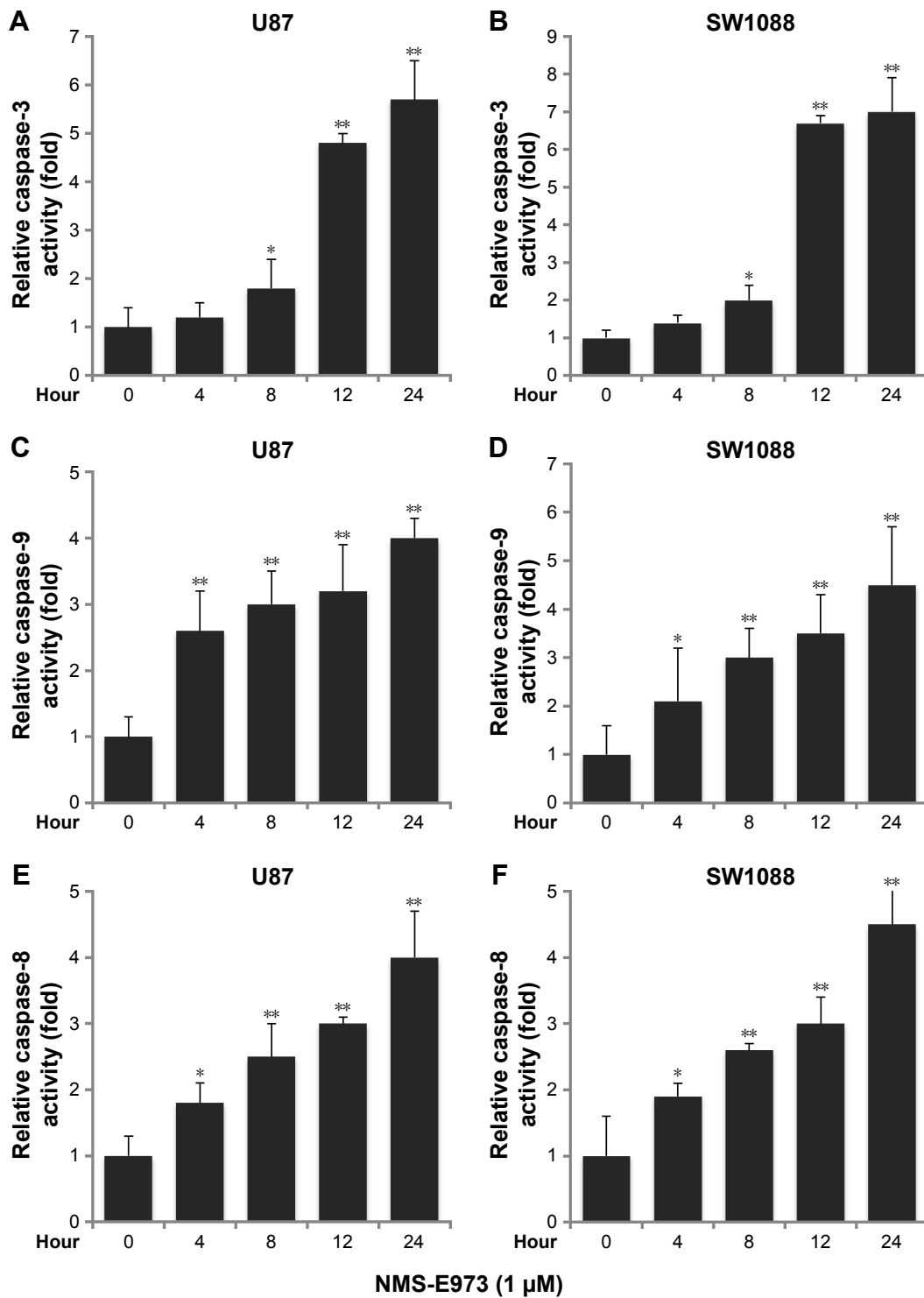


Figure 3 Effect of NMS-E973 on caspase-9, -3, and -8 activation in glioblastoma cells.

Notes: Glioblastoma cells were treated with NMS-E973 (1 μM) at indicated times. Cell-free caspase-3 activities of U87 (A) and SW1088 (B) were analyzed with certain substrates, Ac-LEHD-AFC (caspase-3). Caspase-3 activities of U87 (C) and SW1088 (D) were analyzed with certain substrates, Ac-DEVD-AFC (caspase-9). Caspase-8 activities of U87 (E) and SW1088 (F) were examined with certain substrates, Ac-IETD-AFC (caspase-8). Figure values were calculated as the mean ± SD of three experiments done in total. * $P < 0.01$, ** $P < 0.001$.

assay before and after NMS-E973 treatment. As shown in Figure 4A, mRNA level of *PUMA* was increased to over fivefold after NMS-E973 treatment in U87 cells, while the levels of *NOXA* and *BAD* remained unchanged before and

after NMS-E973 treatment. Further protein expression analysis using Western blot confirmed the induction of *PUMA* by NMS-E973 in U87 cells (Figure 4B). Although we observed the induction of *BID* at mRNA level in both U87 and SW1088

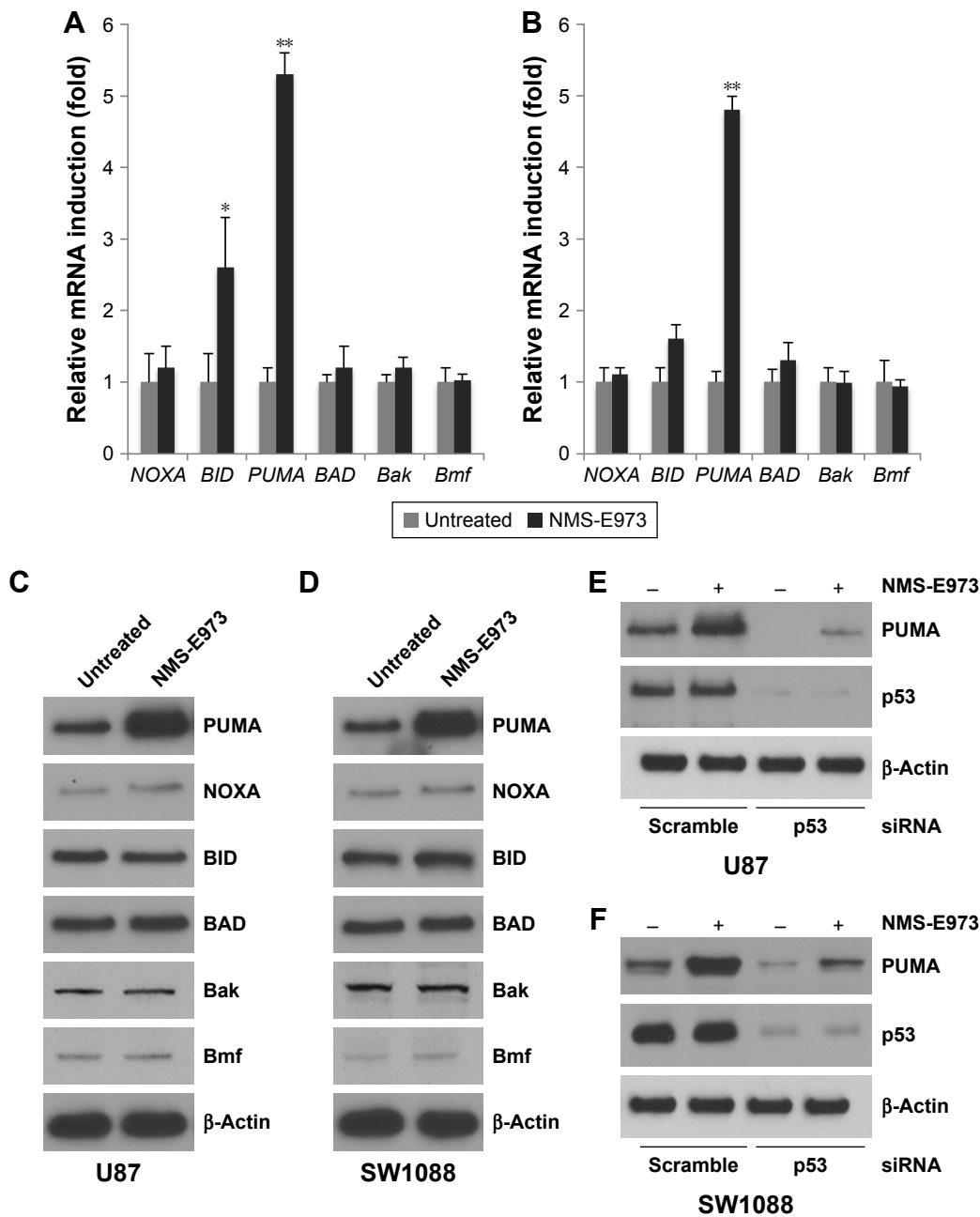


Figure 4 PUMA is induced by NMS-E973 in glioblastoma cells.

Notes: Glioblastoma cells were treated with NMS-E973 (1 μ M) for 24 hours. (A) The mRNA levels of the indicated gene in U87 cells were evaluated by RT-PCR. (B) Expression of the indicated protein in U87 cells was measured by Western blot. (C) The mRNA levels of the indicated gene in SW1088 cells were evaluated by the RT-PCR. (D) Expression of the indicated protein in SW1088 cells was measured by Western blot. U87 cells (E) or SW1088 cells (F) were transfected with siRNA against p53 prior to NMS-E973 (1 μ M) treatment for 24 hours. Expression of the indicated protein in U87 cells was measured by Western blot. Expression of significant difference: * P <0.01, ** P <0.001.

Abbreviation: RT-PCR, reverse-transcriptase PCR.

cells, we were not able to detect a protein level change before and after NMS-E973 treatment (Figure 4). Moreover using qRT-PCR and Western blot assay, we found that induction of PUMA at both mRNA and protein levels by NMS-E973 also existed in SW1088 cells (Figure 4C and D). Finally, in both the glioblastoma cell lines, siRNA against p53 was used to abrogate p53 expression (Figure 4E and F). We found that the induction of PUMA after NMS-E973 treatment was

significantly suppressed when p53 was silenced (Figure 4E and F).

PUMA is required for NMS-E973-induced apoptosis in glioblastoma cells

To determine the role of PUMA in NMS-E973-induced apoptosis, siRNA against PUMA was employed to suppress PUMA expression in glioblastoma cells. As shown in Figure 5A,

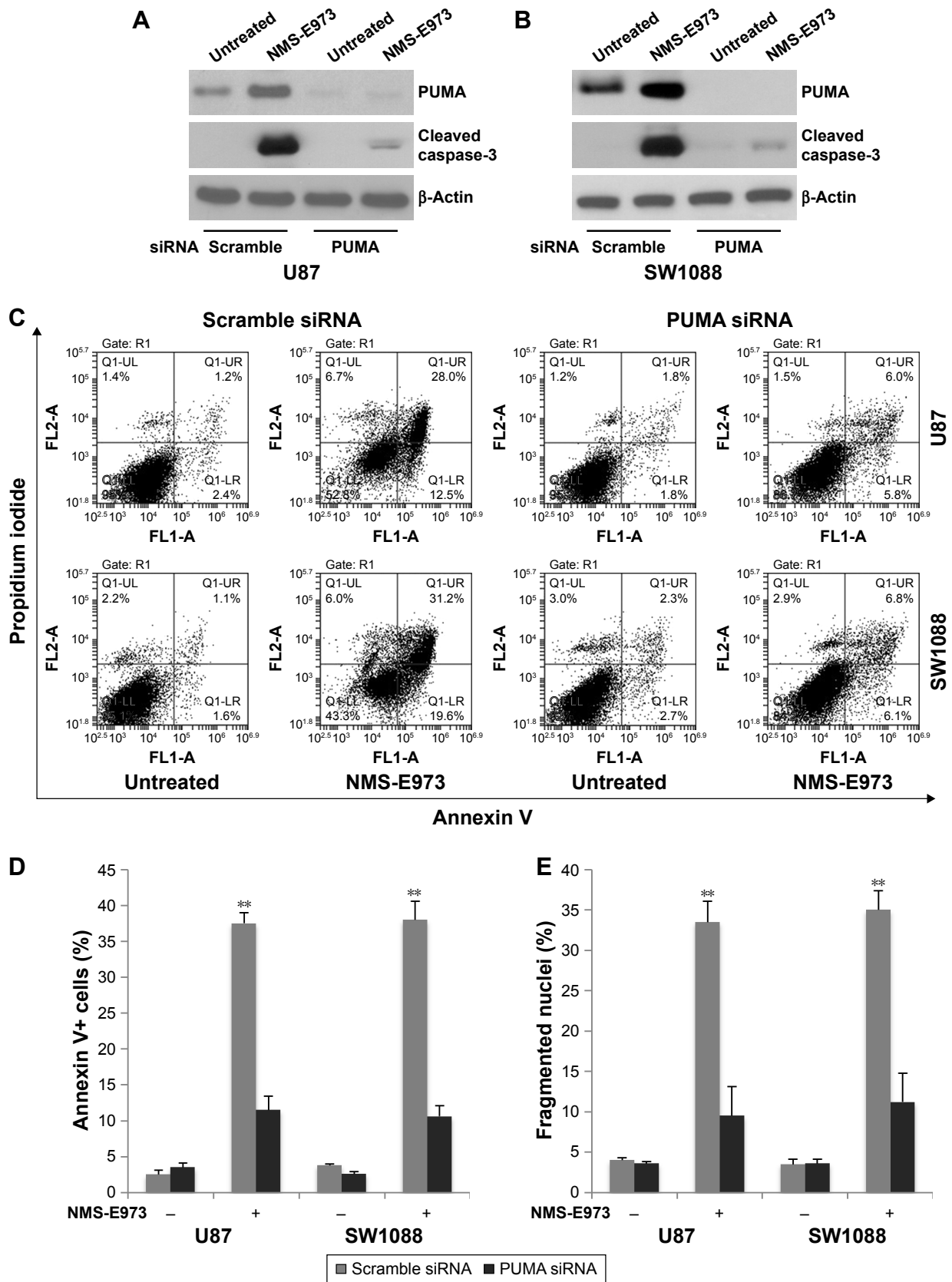


Figure 5 PUMA is required for NMS-E973-induced apoptosis in glioblastoma cells.

Notes: Glioblastoma cells were transfected with either a scrambled siRNA or PUMA siRNA for 24 hours and then treated with NMS-E973 (1 μ M) for 48 hours. Expression of indicated protein in U87 (A) cells and SW1088 (B) cells was measured by Western blot. (C) Representative images of Annexin V/propidium iodide staining in U87 and SW1088 cells with siRNA transfection and following with NMS-E973 (1 μ M) treatment for 48 hours. (D) Annexin V+ cell percentage (indicated in the two right quadrants) was plotted. (E) The condensed and fragmented nuclei were counted in number for apoptosis analysis. Expression of significant difference: ** $P < 0.001$.

PUMA expression was almost completely abolished in U87 cells. At the same time, increasing of cleaved caspase-3 by NMS-E973 treatment was significantly attenuated. Similar results were also found in SW1088 cells (Figure 5B). Moreover, Annexin V/propidium iodide staining and apoptotic cell counting confirmed the negative impact of PUMA knockdown on NMS-E973-induced apoptosis in both U87 and SW1088 cells (Figure 5C–E).

PUMA contributes to the antitumor activities of NMS-E973 in a xenograft model

To determine whether PUMA-mediated apoptosis plays a critical role in the antitumor activity of NMS-E973 *in vivo*, we generated glioblastoma cell lines stably overexpressing shRNA against PUMA using retroviral vectors (U87-PUMA-KD). As shown in Figure 6C, PUMA expression level in U87-PUMA-KD cells was barely detectable compared with parental U87 cells. Then, the wild-type (WT) and PUMA-KD U87 cells were injected into opposite flanks of the same mice to establish xenograft tumors. Mice were then treated with 25 mg/kg NMS-E973 or the vehicle intraperitoneally, and tumor volumes were monitored every 2 days. The WT U87 tumors responded well to NMS-E973 treatment (Figure 6A). In contrast, the PUMA-KD U87 tumors respond poorly to NMS-E973 treatment (Figure 6A). At the end of the experiment, the tumor weight in the WT group was also significantly lower than that in the PUMA-KD group (Figure 6B). Similar to the *in vitro* results, NMS-E973 treatment still had the capacity to induce PUMA expression in WT U87 tumors (Figure 6C). Consistent with NMS-E973-induced apoptosis in cell lines, staining of active caspase-3 and TUNEL were also significantly increased after NMS-E973 treatment in WT U87 tumors, whereas no significant upregulation of these two apoptotic markers in PUMA-KD U87 tumors was observed (Figure 6D–G).

Discussion

Since the late 1990s, much attention has been paid to targeting Hsp90 for cancer therapy. Currently, more than 20 Hsp90 inhibitors have entered clinical trials for use as potential anticancer agents.¹⁷ Similar to the natural product geldanamycin and its less toxic analogs 17-allylamino-17-demethoxygeldanamycin as well as 17-dimethylaminoethylamino-17-demethoxy-geldanamycin, NMS-E973 inhibits the molecular chaperone function of Hsp90 by binding to its ATP-binding site and causing the destabilization of its complexes with client proteins.¹⁸ A previous report also found

the inhibitory role of NMS-E973 on cell proliferation in more than 100 human tumor cell lines, including neuroblastoma cells, SH-SY5Y.¹³ In this study, we demonstrated that NMS-E973 exhibited significant antitumor efficacy in glioblastoma by inhibiting proliferation and colony formation of two human glioblastoma cells *in vitro* and xenograft tumor growth *in vivo*, which is consistent with previous reports showing that inhibition of Hsp90 had significant antitumor efficacy in glioblastoma, including 17-allylamino-17-demethoxygeldanamycin¹⁹ and 17-dimethylaminoethylamino-17-demethoxy-geldanamycin.²⁰ However, considering the frequently observed hepatic toxicity of 17-allylamino-17-demethoxygeldanamycin, gastrointestinal and ocular toxicity of second-generation Hsp90 inhibitors in clinical trials,^{9,21,22} and the low blood–brain barrier permeability of AUY-922,²³ the unique chemical structure and capacity of NMS-E973 to enter into the brain is of potential clinical significance for patients with glioblastoma in future.

Compelling evidence has demonstrated that programmed cell death (apoptosis) is a key procedure in both classic chemoradiotherapy and targeted therapy using small molecules against oncogenes directly on tumor cells.²⁴ Evasion of cell death is a hallmark of cancer and an important contributor to therapeutic resistance.^{25,26} Through Annexin V/propidium iodide staining, condensed chromatin and micronucleation following nuclear staining with Hoechst 33258, cell counting, and caspase-3, -8, and -9 activation detection, we confirmed the contribution of apoptosis toward the antitumor efficacy of NMS-E973 against glioblastoma.

When further exploring the proapoptotic contributor regarding NMS-E973-induced apoptosis in glioblastoma, we found that NMS-E973 treatment leads to a strong induction of the proapoptotic Bcl-2 member PUMA in multiple glioblastoma cell lines *in vitro* and *in vivo*. Silencing of p53 with siRNA significantly abrogated the induction of PUMA by NMS-E973 in both the glioblastoma cell lines. PUMA belongs to the BH3-only subgroup of Bcl-2 family proteins and has been shown to be an apoptotic inducer by directly activating Bax/Bak following the neutralization of other antiapoptotic Bcl-2 family members, thus promoting mitochondrial dysfunction and caspase activation.^{27–29} Our data demonstrated that PUMA is required for NMS-E973-induced apoptosis in glioblastoma cells *in vitro* and also demonstrated the antitumor efficacy of NMS-E973 in xenograft model *in vivo*, which is consistent with the indispensable role played by PUMA by inhibition of Hsp90 with 17AAG in colorectal cancer.³⁰ Since induction of PUMA after p53 knockdown was still observed in cell-based assays, other

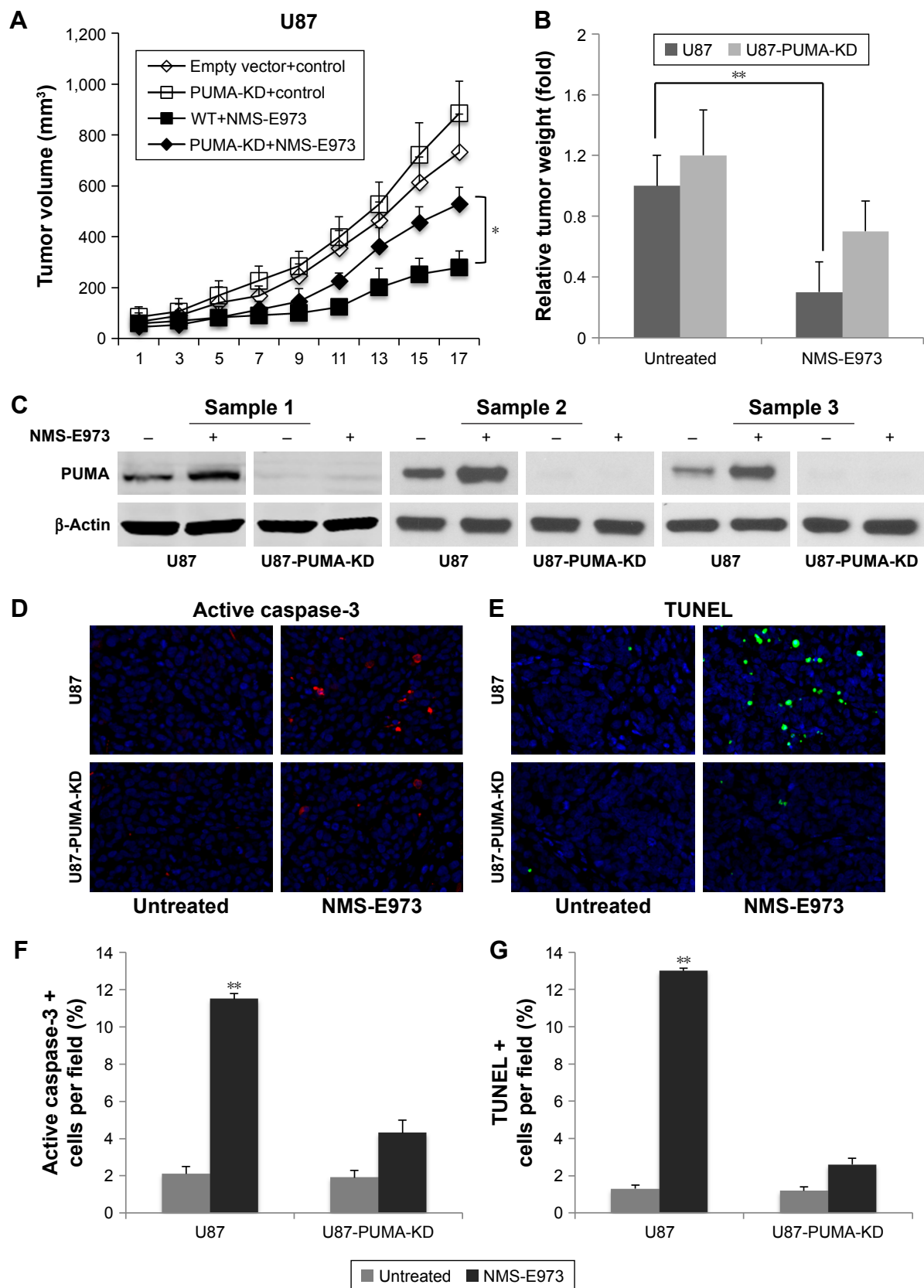


Figure 6 PUMA contributes to the antitumor activities of NMS-E973 in a xenograft model.

Notes: (A) Tumor volume at indicated time points after treatment was calculated and plotted (n=6 in each group). (B) The relative weight of tumor at the end of the experiment. (C) The indicated proteins were analyzed by Western blotting in representative tumors. (D) Representative images of paraffin-embedded tumor sections were analyzed by active caspase-3 staining. (E) Representative images of paraffin-embedded tumor sections analyzed by TUNEL staining. (F) Quantification graph regarding (D). (G) Quantification graph regarding (E). Expression of significant difference: * $P < 0.01$, ** $P < 0.001$.

potential mechanism of induction of PUMA by NMS-E973 was worthy to explore in the future, such as Keap 1,³¹ NF- κ B,³² and p73.³³

In conclusion, our study demonstrates a potential therapeutic strategy of using NMS-E973 against glioblastoma by proving the antitumor mechanism of action of NMS-E973 via PUMA-mediated apoptosis. These findings are in line with other recent findings in which PUMA mediates the apoptotic response to Hsp90 inhibitors. Therefore, induction of PUMA may be a predictor for a favorable response to NMS-E973. We believe this knowledge has important implications for the future development of Hsp90 inhibitors.

Conclusion

Our results demonstrated that Hsp90 inhibitor NMS-E973 can be a therapeutic strategy for glioblastoma treatment, and we also establish the importance of the PUMA in NMS-E973-induced cell killing, which can have important implications with regard to its clinical applications.

Disclosure

The authors report no conflicts of interest in this work.

References

- Siegel RL, Miller KD, Jemal A. Cancer statistics, 2016. *CA Cancer J Clin*. 2016;66(1):7–30.
- Northcott PA. Cancer: keeping it real to kill glioblastoma. *Nature*. 2017; 547(7663):291–292.
- Wong ET, Hess KR, Gleason MJ, et al. Outcomes and prognostic factors in recurrent glioma patients enrolled onto phase II clinical trials. *J Clin Oncol*. 1999;17(8):2572–2578.
- Carson KA, Grossman SA, Fisher JD, Shaw EG. Prognostic factors for survival in adult patients with recurrent glioma enrolled onto the new approaches to brain tumor therapy CNS consortium phase I and II clinical trials. *J Clin Oncol*. 2007;25(18):2601–2606.
- Balmaceda C, Peereboom D, Pannullo S, et al. Multi-institutional phase II study of temozolomide administered twice daily in the treatment of recurrent high-grade gliomas. *Cancer*. 2008;112(5):1139–1146.
- da Fonseca CO, Schwartzmann G, Fischer J, et al. Preliminary results from a phase I/II study of perillyl alcohol intranasal administration in adults with recurrent malignant gliomas. *Surg Neurol*. 2008;70(3): 259–266; discussion 266–267.
- Meyer MA. Malignant gliomas in adults. *N Engl J Med*. 2008;359(17): 1850; author reply 1850.
- Miller TE, Liao BB, Wallace LC, et al. Transcription elongation factors represent in vivo cancer dependencies in glioblastoma. *Nature*. 2017; 547(7663):355–359.
- Neckers L, Workman P. Hsp90 molecular chaperone inhibitors: are we there yet? *Clin Cancer Res*. 2012;18(1):64–76.
- Pick E, Kluger Y, Giltnane JM, et al. High HSP90 expression is associated with decreased survival in breast cancer. *Cancer Res*. 2007;67(7): 2932–2937.
- Song CH, Park SY, Eom KY, et al. Potential prognostic value of heat-shock protein 90 in the presence of phosphatidylinositol-3-kinase overexpression or loss of PTEN, in invasive breast cancers. *Breast Cancer Res*. 2010;12(2):R20.
- Chen MH, Chiang KC, Cheng CT, et al. Antitumor activity of the combination of an HSP90 inhibitor and a PI3K/mTOR dual inhibitor against cholangiocarcinoma. *Oncotarget*. 2014;5(9):2372–2389.
- Fogliatto G, Gianellini L, Brasca MG, et al. NMS-E973, a novel synthetic inhibitor of Hsp90 with activity against multiple models of drug resistance to targeted agents, including intracranial metastases. *Clin Cancer Res*. 2013;19(13):3520–3532.
- Brasca MG, Mantegani S, Amboldi N, et al. Discovery of NMS-E973 as novel, selective and potent inhibitor of heat shock protein 90 (Hsp90). *Bioorg Med Chem*. 2013;21(22):7047–7063.
- Barbagallo I, Parenti R, Zappala A, et al. Combined inhibition of Hsp90 and heme oxygenase-1 induces apoptosis and endoplasmic reticulum stress in melanoma. *Acta Histochem*. 2015;117(8):705–711.
- Zheng X, He K, Zhang L, Yu J. Crizotinib induces PUMA-dependent apoptosis in colon cancer cells. *Mol Cancer Ther*. 2013;12(5): 777–786.
- Workman P, Burrows F, Neckers L, Rosen N. Drugging the cancer chaperone HSP90: combinatorial therapeutic exploitation of oncogene addiction and tumor stress. *Ann N Y Acad Sci*. 2007;1113:202–216.
- Kamal A, Thao L, Sensintaffar J, et al. A high-affinity conformation of Hsp90 confers tumour selectivity on Hsp90 inhibitors. *Nature*. 2003; 425(6956):407–410.
- Sauvageot CM, Weatherbee JL, Kesari S, et al. Efficacy of the HSP90 inhibitor 17-AAG in human glioma cell lines and tumorigenic glioma stem cells. *Neuro Oncol*. 2009;11(2):109–121.
- Kim JG, Lee SC, Kim OH, et al. HSP90 inhibitor 17-DMAG exerts anticancer effects against gastric cancer cells principally by altering oxidant-antioxidant balance. *Oncotarget*. 2017;8(34):56473–56489.
- Jhaveri K, Taldone T, Modi S, Chiosis G. Advances in the clinical development of heat shock protein 90 (Hsp90) inhibitors in cancers. *Biochim Biophys Acta*. 2012;1823(3):742–755.
- Ying W, Du Z, Sun L, et al. Ganetespib, a unique triazolone-containing Hsp90 inhibitor, exhibits potent antitumor activity and a superior safety profile for cancer therapy. *Mol Cancer Ther*. 2012;11(2):475–484.
- Gaspar N, Sharp SY, Eccles SA, et al. Mechanistic evaluation of the novel HSP90 inhibitor NVP-AUY922 in adult and pediatric glioblastoma. *Mol Cancer Ther*. 2010;9(5):1219–1233.
- Fulda S, Debatin KM. Extrinsic versus intrinsic apoptosis pathways in anticancer chemotherapy. *Oncogene*. 2006;25(34):4798–4811.
- Hanahan D, Weinberg RA. Hallmarks of cancer: the next generation. *Cell*. 2011;144(5):646–674.
- Vogelstein B, Kinzler KW. Cancer genes and the pathways they control. *Nat Med*. 2004;10(8):789–799.
- Yu J, Zhang L. Apoptosis in human cancer cells. *Curr Opin Oncol*. 2004;16(1):19–24.
- Ming L, Wang P, Bank A, Yu J, Zhang L. PUMA dissociates Bax and Bcl-X(L) to induce apoptosis in colon cancer cells. *J Biol Chem*. 2006; 281(23):16034–16042.
- Youle RJ, Strasser A. The BCL-2 protein family: opposing activities that mediate cell death. *Nat Rev Mol Cell Biol*. 2008;9(1):47–59.
- He K, Zheng X, Zhang L, Yu J. Hsp90 inhibitors promote p53-dependent apoptosis through PUMA and Bax. *Mol Cancer Ther*. 2013;12(11):2559–2568.
- Cazanave SC, Wang X, Zhou H, et al. Degradation of Keap1 activates BH3-only proteins Bim and PUMA during hepatocyte lipoapoptosis. *Cell Death Diff*. 2014;21(8):1303–1312.
- Wang P, Qiu W, Dudgeon C, et al. PUMA is directly activated by NF- κ B and contributes to TNF- α -induced apoptosis. *Cell Death Diff*. 2009;16(9):1192–1202.
- Ming L, Sakaida T, Yue W, Jha A, Zhang L, Yu J. Sp1 and p73 activate PUMA following serum starvation. *Carcinogenesis*. 2008;29(10): 1878–1884.

OncoTargets and Therapy

Dovepress

Publish your work in this journal

OncoTargets and Therapy is an international, peer-reviewed, open access journal focusing on the pathological basis of all cancers, potential targets for therapy and treatment protocols employed to improve the management of cancer patients. The journal also focuses on the impact of management programs and new therapeutic agents and protocols on

patient perspectives such as quality of life, adherence and satisfaction. The manuscript management system is completely online and includes a very quick and fair peer-review system, which is all easy to use. Visit <http://www.dovepress.com/testimonials.php> to read real quotes from published authors.

Submit your manuscript here: <http://www.dovepress.com/oncotargets-and-therapy-journal>